# Continuous wave laser operation in Nd:GGG depressed tubular cladding waveguides produced by inscription of femtosecond laser pulses

**Hongliang Liu,[1] Yuechen Jia,[1] Feng Chen,[1,*] and Javier R. Vázquez de Aldana[2]**

[1]*School of Physics, State Key Laboratory of Crystal Materials and Key Laboratory of Particle Physics and Particle Irradiation (Ministry of Education), Shandong University, Jinan 250100, China*
[2]*Laser Microprocessing Group, Universidad de Salamanca, Salamanca 37008, Spain*
**drfchen@sdu.edu.cn*

**Abstract:** Depressed tubular cladding waveguides have been produced in Nd:GGG crystals by using multiple inscription with femtosecond (fs) laser pulses. The guiding cores are located inside the tubular regions with cross-section diameters of 90-150 μm, which are surrounded by fs-laser induced low-refractive-index tracks. At room temperature continuous wave (cw) laser oscillations at wavelength of ~1063 nm have been realized through the optical pump at 808 nm. The slope efficiency of the cladding waveguide lasers is as high as 44.4% and the maximum output power at 1063 nm is 209 mW, which shows superior laser performance to the Type II stress induced Nd:GGG waveguides.



**OCIS codes:** (230.7370) Waveguides; (140.3390) Laser materials processing; (130.3120) Integrated optics devices.

## References and links

1. R. R. Gattass and E. Mazur, "Femtosecond laser micromachining in transparent materials," Nat. Photonics **2**(4), 219–225 (2008).
2. K. M. Davis, K. Miura, N. Sugimoto, and K. Hirao, "Writing waveguides in glass with a femtosecond laser," Opt. Lett. **21**(21), 1729–1731 (1996).
3. J. Burghoff, S. Nolte, and A. Tünnermann, "Origins of waveguiding in femtosecond laser-structured $LiNbO_3$," Appl. Phys., A Mater. Sci. Process. **89**(1), 127–132 (2007).
4. M. Ams, G. D. Marshall, P. Dekker, J. Piper, and M. Withford, "Ultrafast laser written active devices," Laser Photonics Rev. **3**(6), 535–544 (2009).
5. C. Grivas, "Optically pumped planar waveguide lasers, Part I: Fundamentals and fabrication techniques," Prog. Quantum Electron. **35**(6), 159–239 (2011).
6. D. G. Lancaster, S. Gross, H. Ebendorff-Heidepriem, K. Kuan, T. M. Monro, M. Ams, A. Fuerbach, and M. J. Withford, "Fifty percent internal slope efficiency femtosecond direct-written $Tm^{3+}$:ZBLAN waveguide laser," Opt. Lett. **36**(9), 1587–1589 (2011).
7. R. Mary, S. J. Beecher, G. Brown, R. R. Thomson, D. Jaque, S. Ohara, and A. K. Kar, "Compact, highly efficient ytterbium doped bismuthate glass waveguide laser," Opt. Lett. **37**(10), 1691–1693 (2012).
8. J. Siebenmorgen, K. Petermann, G. Huber, K. Rademaker, S. Nolte, and A. Tunnermann, "Femtosecond laser written stress-induced Nd:$Y_3Al_5O_{12}$ (Nd:YAG) channel waveguide laser," Appl. Phys. B **97**(2), 251–255 (2009).
9. J. Siebenmorgen, T. Calmano, K. Petermann, and G. Huber, "Highly efficient Yb:YAG channel waveguide laser written with a femtosecond-laser," Opt. Express **18**(15), 16035–16041 (2010).
10. A. Okhrimchuk, V. Mezentsev, A. Shestakov, and I. Bennion, "Low loss depressed cladding waveguide inscribed in YAG:Nd single crystal by femtosecond laser pulses," Opt. Express **20**(4), 3832–3843 (2012).
11. G. A. Torchia, A. Rodenas, A. Benayas, E. Cantelar, L. Roso, and D. Jaque, "Highly efficient laser action in femtosecond-written Nd:yttrium aluminum garnet ceramic waveguides," Appl. Phys. Lett. **92**(11), 111103 (2008).
12. T. Calmano, A. G. Paschke, J. Siebenmorgen, S. T. Fredrich-Thornton, H. Yagi, K. Petermann, and G. Huber, "Characterization of an Yb:YAG ceramic waveguide laser, fabricated by the direct femtosecond-laser writing technique," Appl. Phys. B **103**(1), 1–4 (2011).
13. Y. Tan, F. Chen, J. R. Vázquez de Aldana, G. A. Torchia, A. Benayas, and D. Jaque, "Continuous wave laser generation at 1064 nm in femtosecond laser inscribed Nd:$YVO_4$ channel waveguides," Appl. Phys. Lett. **97**(3), 031119 (2010).

#179247 - $15.00 USD Received 5 Nov 2012; revised 4 Jan 2013; accepted 17 Jan 2013; published 18 Jan 2013

14. Y. Tan, A. Rodenas, F. Chen, R. R. Thomson, A. K. Kar, D. Jaque, and Q. M. Lu, "70% slope efficiency from an ultrafast laser-written Nd:$GdVO_4$ channel waveguide laser," Opt. Express **18**(24), 24994–24999 (2010).
15. H. Liu, Y. Jia, J. R. Vázquez de Aldana, D. Jaque, and F. Chen, "Femtosecond laser inscribed cladding waveguides in Nd:YAG ceramics: fabrication, fluorescence imaging and laser performance," Opt. Express **20**(17), 18620–18629 (2012).
16. Y. Ren, G. Brown, A. Ródenas, S. Beecher, F. Chen, and A. K. Kar, "Mid-infrared waveguide lasers in rare-earth-doped YAG," Opt. Lett. **37**(16), 3339–3341 (2012).
17. Y. Jia, F. Chen, and J. R. Vázquez de Aldana, "Efficient continuous-wave laser operation at 1064 nm in Nd:$YVO_4$ cladding waveguides produced by femtosecond laser inscription," Opt. Express **20**(15), 16801–16806 (2012).
18. Y. Jia, J. R. Vázquez de Aldana, C. Romero, Y. Ren, Q. Lu, and F. Chen, "Femtosecond-laser-inscribed $BiB_3O_6$ nonlinear cladding waveguide for second-harmonic generation," Appl. Phys. Express **5**(7), 072701 (2012).
19. N. Dong, F. Chen, and J. R. Vázquez de Aldana, "Efficient second harmonic generation by birefringent phase matching in femtosecond laser inscribed KTP cladding waveguides," Phys. Status Solidi (RRL) **6**(7), 306–308 (2012).
20. Z. Jia, X. Tao, C. Dong, X. Cheng, W. Zhang, F. Xu, and M. Jiang, "Study on crystal growth of large size $Nd^{3+}$:$Gd_3Ga_5O_{12}$ ($Nd^{3+}$:GGG) by Czochralski method," J. Cryst. Growth **292**(2), 386–390 (2006).
21. F. Chen, "Micro-and submicrometric waveguiding structures in optical crystals produced by ion beams for photonic applications," Laser Photonics Rev. **6**(5), 622–640 (2012).
22. S. J. Field, D. C. Hanna, A. C. Large, D. P. Shepherd, A. C. Tropper, P. J. Chandler, P. D. Townsend, and L. Zhang, "Ion-implanted Nd:GGG channel waveguide laser," Opt. Lett. **17**(1), 52–54 (1992).
23. Y. Yao, N. Dong, F. Chen, S. K. Vanga, and A. A. Bettiol, "Proton beam writing of Nd:GGG crystals as new waveguide laser sources," Opt. Lett. **36**(21), 4173–4175 (2011).
24. C. Zhang, N. N. Dong, J. Yang, F. Chen, J. R. Vázquez de Aldana, and Q. M. Lu, "Channel waveguide lasers in Nd:GGG crystals fabricated by femtosecond laser inscription," Opt. Express **19**(13), 12503–12508 (2011).
25. R. Ramponi, R. Osellame, and M. Marangoni, "Two straightforward methods for the measurement of optical losses in planar waveguides," Rev. Sci. Instrum. **73**(3), 1117–1120 (2002).

## 1. Introduction

Femtosecond (fs) laser inscription has been proved to be a powerful and unique technique to fabricate optical waveguides in various transparent optical materials [1–4]. In the active waveguides, the mode volumes are strongly compressed owing to the small scales of dimensions, which leads to an optimum spatial overlap between pump and laser beams. As a result, waveguide lasers possess some attractive advantages such as low lasing thresholds and comparable efficiencies with respect to bulk lasers, which make them as promising integrated light sources for the construction of multifunctional photonic devices [5]. By using the active waveguides produced by the inscription of fs laser pulses, people have developed efficient micro-laser systems in a couple of laser materials, such as Tm:ZBLAN glasses [6], Yb:bismuthate glass [7], rare-earth ion doped YAG crystals [8–10], ceramics [11,12], and vanadate crystals [13,14]. For crystalline materials, the double-line technique has already been applied to form stress-induced waveguides (so-called Type II configuration) [3,8]. Since the fs-laser induced tracks show usually reduced refractive index, compared with the bulks, to use multiple filaments by more fs laser scans may be a solution to further improve the guidance of the light within the waveguide core, and at same time, the fabricated waveguides may support light guidance at longer wavelengths provided the scale of the waveguides increases. Recently, the depressed tubular cladding waveguides with circular cross sections have been manufactured in laser materials (such as Nd:YAG crystals [10] and ceramics [15], Tm:YAG ceramics [16], Nd:$YVO_4$ crystals [17], and Tm:ZBLAN glass [6]) as well as in nonlinear crystals (such as $BiB_3O_6$ [18] and $KTiOPO_4$ [19]). The laser oscillations or nonlinear responses of these crystalline cladding waveguides have shown excellent performances.

Cubic Nd-doped gadolinium gallium garnet (Nd:$Gd_3Ga_5O_{12}$ or Nd:GGG) is one of the well-known gain media for solid state laser systems [20]. Channel waveguides have been fabricated in Nd:GGG crystals by ion beam irradiation [21] (masked He ion implantation [22], proton beam writing [23] and double-line fs-laser inscription [24]). In this work, we focus on the fabrication of Nd:GGG circular cladding waveguides constructed with more fs-laser tracks as well on the comparison of the guiding properties and laser performances of the waveguides with these different volume configurations.

#179247 - $15.00 USD Received 5 Nov 2012; revised 4 Jan 2013; accepted 17 Jan 2013; published 18 Jan 2013

## 2. Experiments in details

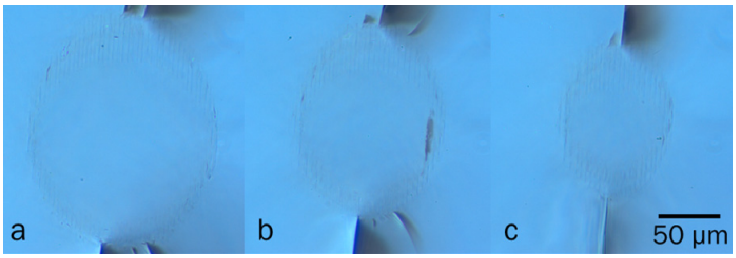


Fig. 1. Microscope images of the fs-laser inscribed Nd:GGG crystals of the depressed tubular cladding waveguides with diameters of (a) 150, (b) 120 and (c) 90 μm.

The Nd:GGG crystal samples (doped by 1 at. % $Nd^{3+}$ ions, obtained from Atom Optics Co. Ltd, Shanghai, China) were cut with sizes of 8 × 8 × 2 $mm^3$. The circular depressed cladding waveguides were produced by using the laser facility of the Universidad de Salamanca, Spain. A Ti:Sapphire regenerative amplifier (Spitfire, Spectra Physics, USA) was used as laser source. It delivered, at 1 kHz repetition rate, linearly-polarized pulses of 120 fs (intensity FWHM) and 795 nm central wavelength. The maximum available pulse energy was 1 mJ but it was reduced with a calibrated neutral density filter placed after a half-wave plate and a linear polarizer, in order to get a fine control of the incident energy.

In order to fabricate the tubular cladding waveguides the pulse energy was set to 2.1 μJ and the laser beam was focused with a 40 × microscope objective (N.A. ~0.65) at 200 μm beneath one of the 8 × 4 $mm^2$ surfaces. The sample was scanned at a constant velocity of 500 μm/s in the direction parallel to the 8-mm edge, producing a damage line along the sample. The procedure was repeated at different depths of the sample, following the desired circular geometry, with a lateral separation of 3 μm between each two adjacent tracks. Three tubular-shape structures with diameters of 150, 120 and 90 μm were fabricated with this technique (see Figs. 1(a)-1(c) for images of the cross sections). Some cracks at the surroundings of the waveguides are observed at this irradiation conditions due to the large stress induced in the crystal, but they do not affect the waveguide core.

To obtain the maximum changes of refractive index of the waveguides, we measured the N. A. of the waveguides and used the formula reported in [8]. The maximum refractive index change $\Delta n$ for the cladding waveguides was estimated to be 2.5 × $10^{-3}$. This value was in good agreement with those of other cladding waveguides [10,17–19], although the method itself was a rough estimation.

The losses of the waveguides were measured at wavelength of 632.8 nm with a He-Ne laser as light source by the back-reflection method [25] for the cladding waveguides. This technique was first designed for planar waveguide loss measurement, but it is also successful for large-scale cladding waveguides. For the depressed cladding waveguides with cross-section diameters of 150, 120 and 90 μm, the propagation losses were determined to be ~1.7 dB/cm, 2.0 dB/cm and 2.5 dB/cm, respectively. In the present case, the difference of losses between TE and TM polarized modes are within 5%.

The cw waveguide laser-operation experiments were performed by using the end pumping system at room temperature. A tunable cw Ti:Sapphire laser (Coherent MBR 110, USA) generated a polarized light pump beam at 808 nm. A spherical convex lens with focal length of 25 mm was used to couple the pump laser beam into the waveguide. To achieve the Fabry-Perot cavity for the 1.06 μm laser emission in the waveguides, two dielectric mirrors were butt-coupled to the two polished end facets (the input one with a high reflectivity (>99%) at 1.06 μm and high transmission (98%) at 808 nm and the output one with reflectivity of 40% at 1.06 μm and >99% at 808 nm. The generated waveguide lasers were collected with a 20 × microscope objective lens (N.A. = 0.4) and imaged by an IR CCD camera through an aperture. A spectrometer was used to analyze the emission spectra of the generated laser beam.

#179247 - $15.00 USD Received 5 Nov 2012; revised 4 Jan 2013; accepted 17 Jan 2013; published 18 Jan 2013

## 3. Results and discussion

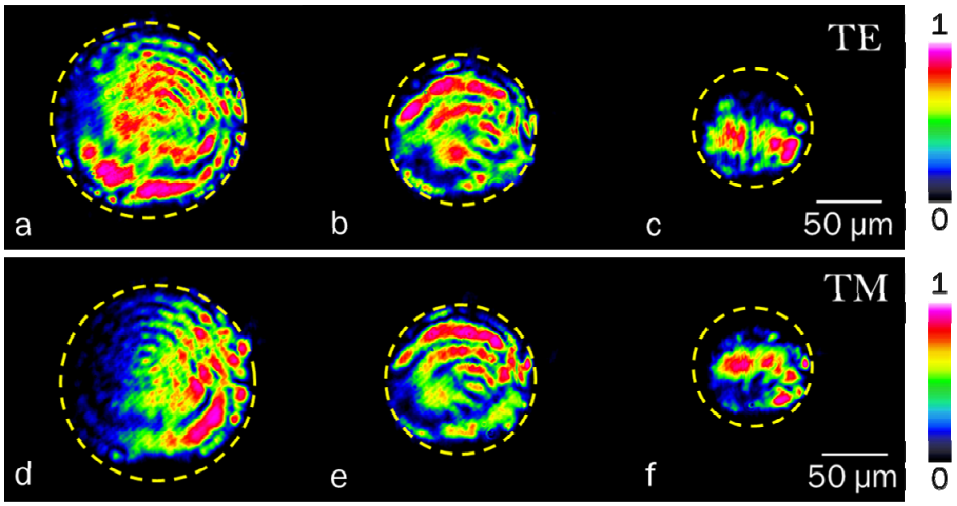


Fig. 2. Near field intensity distributions of the depressed cladding waveguides with diameters of 150, 120 and 90 μm at 632.8 nm, respectively: (a), (b) and (c) for the TE modes and (d), (e) and (f) for the TM modes. The dashed lines indicate the spatial locations of the fs-laser induced damage tracks.

Figures 2(a)-2(c) and 2(d)-2(f) depict the TE and TM polarized modal profiles of the depressed cladding waveguides exhibited highly multimode features, respectively. The large diameters of 90-150 μm of the circular cross section of the cladding waveguides are considered to be the main reason for the multiple modal properties of the structures. As one can see, the boundaries of all the three cladding waveguides are in good agreement with the respective geometries of the structures. In addition, it is also found that the waveguides support guidance in both transverse polarizations of TE and TM as the difference of the propagation losses between TE and TM polarized light is less than 5% as the TM polarized modal profiles were shown in Figs. 2(d), 2(e) and 2(f). This is significantly different with the double-line stress induced Nd:GGG [24] or Nd:YAG [8] cubic crystal waveguides, which are only with guidance along TE polarizations.

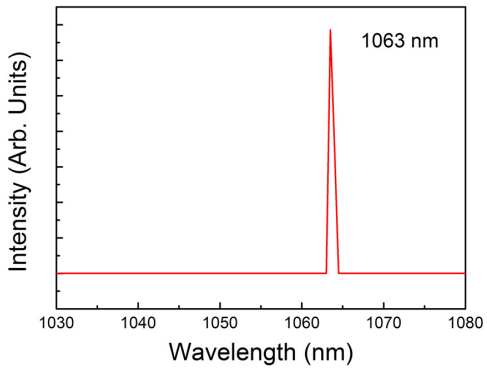


Fig. 3. Typical laser emission spectrum from the fs-laser inscribed Nd:GGG depressed cladding waveguides. Peak position stays at 1063 nm and the FWHM is 0.6 nm.

After knowing the guidance properties of the waveguides at 632.8 nm, we have evaluated their potential use as integrated laser sources by means of end-coupling experiments. Figure 3 depicts the typical laser emission spectrum from the fs laser inscribed Nd:GGG depressed cladding waveguides, when the absorbed power is above the lasing threshold. The central

#179247 - $15.00 USD Received 5 Nov 2012; revised 4 Jan 2013; accepted 17 Jan 2013; published 18 Jan 2013

wavelength of the laser emission from the cladding waveguide is at 1063 nm, which corresponds to the main fluorescence of $^4F_{3/2} \rightarrow {}^4I_{11/2}$ transition in the $Nd^{3+}$ ions, with a FWHM of ~0.6 nm.

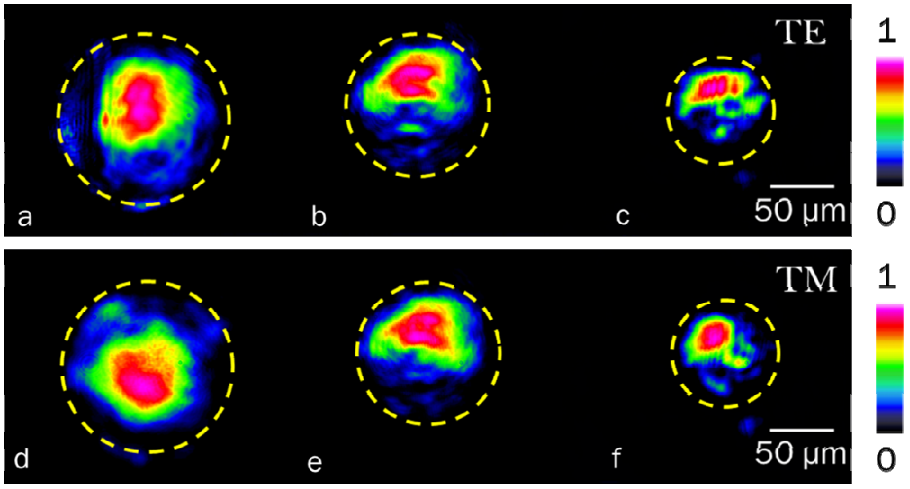


Fig. 4. Waveguide laser modal distributions at 1063 nm of the depressed cladding waveguides with diameters of 150 μm, 120 μm and 90 μm under 808 nm optical pump: (a), (b) and (c) for the TE polarization and (d), (e) and (f) for the TM polarization, respectively.

From Figs. 4(a)-4(f), we can see the spatial intensity distributions of the output laser at both TE and TM modes generated in the depressed cladding waveguides with diameters of 150 μm, 120 μm and 90 μm at 1063 nm under 808 nm optical pumping, respectively. The infrared profiles of the waveguide lasers (Figs. 4(a)-4(f)) show obviously reduced mode numbers (showing profiles of nearly fundamental modes by careful adjustment of the components of the mode coupling system to focus the main modal field in $TE_{00}$ or $TM_{00}$). It should be pointed out that the TM modes of the waveguide lasers are very similar to the TE modes of the cladding waveguides. In Type II stress-induced Nd:GGG [24] or Nd:YAG [8] waveguides, lasing were generated only along the TM polarization. In this sense, the cladding waveguide configuration seems to be more advantageous since the waveguide laser systems could be pumped with non-polarized diode lasers.

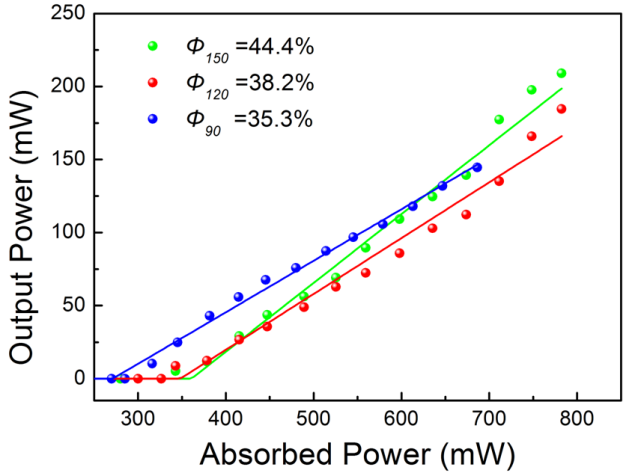


Fig. 5. Cw waveguide (TM mode) laser output power at 1063 nm as a function of the absorbed power at 808 nm. The green, red and blue lines stand for the data of the depressed cladding waveguides with diameters of 150 μm, 120 μm and 90 μm, respectively.

#179247 - $15.00 USD Received 5 Nov 2012; revised 4 Jan 2013; accepted 17 Jan 2013; published 18 Jan 2013

Figure 5 shows the output laser powers (at wavelength of 1063 nm) as a function of the absorbed pump powers at 808 nm generated in the Nd:GGG cladding waveguides along TM polarization with diameter of 150 μm, 120 μm and 90 μm at room temperature, respectively. During the calculation of the absorbed powers and the output powers, we have considered the coupling efficiency of the pump laser, and the transmittance and reflectivity of the optical elements (e.g., microscope lenses) in the end-coupling experiment [24]. From the linear fit of the experimental data, for the depressed cladding waveguides in the Nd:GGG crystals, the lasing thresholds are $P_{150,th}$ ≈360 mW, $P_{120,th}$ ≈348 mW and $P_{90,th}$ ≈270 mW, and the extracted slope efficiencies of these three waveguides are $\Phi_{150}$ ≈44.4%, $\Phi_{120}$ ≈38.2% and $\Phi_{90}$ ≈35.3%, corresponding to optical-to-optical conversion efficiency of $\eta_{150}$ ≈26.7%, $\eta_{120}$ ≈23.5% and $\eta_{90}$ ≈21.8%, respectively. Another different performance is that the maximum output power is $P_{150,M}$ ≈209 mW when the absorbed power climbs at 792 mW. By analysis of the data from Fig. 5, we could conclude that the cladding waveguides with larger diameters have higher output laser powers than the smaller volume waveguide. In addition, the round-trip cavity loss exponential factor $\delta$ and the effective pump area $A_{eff}$ of the waveguide laser system have impacts on the lasing threshold $P_{th}$ as the $P_{th} \propto \delta \cdot A_{eff}$ [5]. It is reasonable that the smaller-diameter cladding waveguides possess lower lasing thresholds with lower coupling efficiency. In addition, we found that the TE polarized waveguide lasers show similar features with the TM modes. The difference of maximum output powers between TE and TM mode waveguide lasers are less than 10%, which is significantly different from the dual-line stress-induced waveguides in Nd:GGG [24]. Moreover, the depressed cladding waveguides with larger volume owns higher slope efficiency and higher output laser power, and the large cross sections of the cladding waveguides with circular cross sections is comparable to the multimode fibers of laser diodes system, which is potentially helpful to construct highly efficient fiber-waveguide laser systems for photonic applications.

## 4. Summary

We have fabricated depressed cladding waveguides in Nd:GGG crystals by using fs laser inscription. Cladding waveguide structures were fabricated with circular cross sections of diameters of 90-150 μm with a large number of damage filaments, supporting multi-mode guidance in both the TE and TM polarizations. In addition, cw laser oscillations at wavelength of ~1063 nm have been realized in both types of waveguides by optical pumping at 808 nm. The best performance was obtained for the cladding waveguides with a slope efficiency of 44.4% and a maximum power of 209 mW. These good laser performances suggest that the Nd:GGG cladding waveguides would be promising candidates as integrated light sources.

## Acknowledgments

The work is supported by the National Natural Science Foundation of China (Nos. 11274203 and 11111130200), the Spanish Ministerio de Ciencia e Innovación (MICINN) through Consolider Program SAUUL CSD2007-00013 and project FIS2009-09522. Support from the Centro de Láseres Pulsados (CLPU) is also acknowledged. The authors thank Mr. Q. M. Lu for polishing the sample in this work.

#179247 - $15.00 USD Received 5 Nov 2012; revised 4 Jan 2013; accepted 17 Jan 2013; published 18 Jan 2013